




Cite this: *RSC Adv.*, 2017, 7, 34262

# Monitoring and manipulating single molecule rotors on the Bi(111) surface by the scanning tunneling microscopy

Yu-Bing Tu,  Min-Long Tao, Kai Sun, Chen Ni, Fang Xie and Jun-Zhong Wang\*

We have investigated rotation and manipulation of manganese phthalocyanine (MnPc) molecules on the semimetallic Bi(111) surface by low-temperature scanning tunneling microscopy (STM). At liquid-helium temperature, individual MnPc molecules adsorb flat on the Bi(111) surface but with a slight bend toward the substrate. The in-plane orientation of the MnPc molecule can be changed by 60° by manipulation with the STM tip. At liquid-nitrogen temperature, the isolated MnPc molecules rotate around the central Mn ion because of the weak molecule–semimetal interaction. The MnPc rotor shows a flower-like feature with six lobes corresponding to the six-fold symmetry of Bi(111) lattice. Most importantly, the MnPc rotors can be started or stopped by controlling the intermolecular spacing with the STM tip. These results are important for understanding and controlling the performance of surface-mounted molecular rotors.

Received 18th May 2017  
Accepted 2nd July 2017

DOI: 10.1039/c7ra05611g

rsc.li/rsc-advances

## 1 Introduction

In the past few decades, translational or rotational movement of various molecules on solid surfaces has been intensely investigated because of its important role in nanoscale engineering at the molecular level.<sup>1,2</sup> Significant progress has been made in developing a wealth of synthetic molecular machines, such as motors,<sup>3–5</sup> switches,<sup>6,7</sup> gears,<sup>8</sup> shuttles<sup>9</sup> and even cogwheels.<sup>10,11</sup> As a key component of these machines, molecular rotors can be defined as molecular systems in which a molecule or part of a molecule rotates against another part of the molecule or a surface.<sup>2</sup> The rotational motion can be driven by thermal energy,<sup>12–15</sup> photons,<sup>16</sup> or electrons.<sup>17</sup> Molecular rotors mounted on solid surfaces have the advantage of accessibility and they are easily organized owing to the reduced dimensions.<sup>18</sup> For instance, rotation of porphyrin and sulfide molecules has been often observed and analyzed.<sup>19–21</sup> Thus, investigating the structure and properties of molecular rotors is necessary for applications in nanotechnology.

Once mounted on a surface, molecular rotors can be easily characterized by scanning tunneling microscope (STM), because it has the ability to not only position the molecular rotors with atomic scale precision but also track the motion of molecules.<sup>22</sup> However, the rotation is too fast to be imaged separately by conventional STM, because it's an intrinsically slow technique.<sup>23</sup> To increase the time resolution, an effective approach is to measure the tunneling current variation *versus* time with the feedback loop turned off. This method has been successfully used to study the dynamics of molecular motion.<sup>24–27</sup> In addition,

the STM tip can be used as a mechanical tool to manipulate single atoms and molecules on solid surfaces. For example, it has been reported that the STM tip can help 4-ethylphenyl groups overcome the potential barrier to rotate,<sup>28</sup> and even drive a specially designed molecular rack and pinion.<sup>29</sup>

In the past several years, transition-metal phthalocyanines (TMPcs) have attracted great interest because of their wide applications. Because of their relatively simple and robust structure, TMPcs are considered to be a prototype magnetic molecule. The magnetic properties of transition-metal atoms can be detected by controlling the charge states, spin states, and Kondo effect.<sup>30–32</sup> Intensive efforts have been made to adsorb TMPcs on various solid surfaces, and various self-assembled structures of TMPcs have been formed on solid surfaces.<sup>33–35</sup> However, there have been relatively few studies of the movement or rotation of TMPc on solid surfaces.

In this study, single molecule rotors of MnPc on the Bi(111) surface have been investigated in detail. At liquid-helium (LHe) temperature, individual MnPc molecules adsorbed on the Bi(111) surface have reduced symmetry owing to the bending of two lobes. The in-plane orientation of MnPc can be rotated by 60° driven by STM tip. At liquid-nitrogen (LN<sub>2</sub>) temperature, the isolated MnPc molecules keep rotating around the Mn ion and show a flower-like pattern. Interestingly, this type of single molecule rotor can be started or stopped by changing the intermolecular spacing with the STM tip.

## 2 Methods

All of the experiments were performed using a Unisoku ultra-high vacuum LT-STM system with a base pressure of about  $2 \times 10^{-10}$  mbar. 20 monolayers of Bi were deposited on a Si(111)-7

School of Physical Science and Technology, Southwest University, Chongqing 400715, China. E-mail: jzwangcn@swu.edu.cn



$\times 7$  surface at room temperature. A very smooth Bi(111) film was obtained after subsequent annealing at 400 K. After overnight degassing, MnPc molecules were thermally evaporated onto the Bi(111) substrate from a tantalum boat heated to  $\sim 600$  K. Constant current STM images were obtained at LHe (4.6 K) or LN<sub>2</sub> (78 K) temperatures.

Theoretical calculations were performed based on density functional theory (DFT). The Vienna *ab initio* simulation package (VASP)<sup>36,37</sup> code was used with the Perdew–Burke–Ernzerhof (PBE) generalized gradient approximation (GGA) for exchange–correlation energy,<sup>38</sup> with the projector augmented waves (PAW) method.<sup>39,40</sup> One MnPc molecule was placed on a Bi(111) slab simulated by four layers of a  $6 \times 6$  unit cell. The cutoff energy for the plane waves was 400 eV with only  $\Gamma$ -point sampling. All of the atoms except for the bottom two bismuth layers were fully relaxed until the net force on every atom was less than  $0.04 \text{ eV } \text{\AA}^{-1}$ . Self-consistent spin orbit coupling was considered, and van der Waals correction (DFT-D2 method of Grimme<sup>41</sup>) was taken into account to compare with previous work. The simulated STM image was obtained by the Tersoff–Hamann approximation.<sup>42</sup>

### 3 Results

First, a small amount of MnPc molecules was deposited on the Bi(111) surface. Individual MnPc molecules adsorbed flat on the substrate. Two opposed lobes aligned along the base vector

directions and the other two lobes pointed in the  $\sqrt{3}$  direction of Bi(111) surface [Fig. 1(b)]. From the high-resolution STM image in Fig. 1(c), the MnPc molecule appears as a cross shape with a protrusion at the center, which is consistent with its chemical structure in Fig. 1(a). However, the two vertical lobes of MnPc split into two branches while the horizontal two lobes show no splitting. As a result, the  $C_4$  symmetry of the free MnPc molecule is reduced to  $C_2$  in the STM image. A similar reduction of symmetry has been observed for SnPc on Ag(111).<sup>43</sup>

To investigate the origin of the symmetry reduction, we performed the DFT calculations of optimized geometries of MnPc on Bi(111). The results show that the central Mn ion anchors to the top site of the Bi(111) surface in the minimum energy configuration. Two of the opposing lobes slightly bend toward the substrate, while the other two lobes remain flat, as shown in Fig. 1(d). The simulated STM image is shown in Fig. 1(e), where the two flat lobes split but the two bent lobes show no splitting. The reduction of symmetry is consistent with the STM observation in Fig. 1(c). Moreover, the minimum adsorption energy is  $-2.7 \text{ eV}$ , which is much greater than  $-5.9 \text{ eV}$  for MnPc on Cu(001).<sup>44</sup> The weak interaction indicates that the MnPc molecules on Bi(111) can be easily manipulated by a STM tip, as shown in Fig. 1(f). The in-plane orientation of the MnPc molecule changes by  $60^\circ$  relative to the orientation in Fig. 1(c), when reducing the scanning bias.

With increasing coverage, individual MnPc molecules assemble into one-dimensional molecular chains and two-dimensional domains. Fig. 2(a) shows a STM image of several

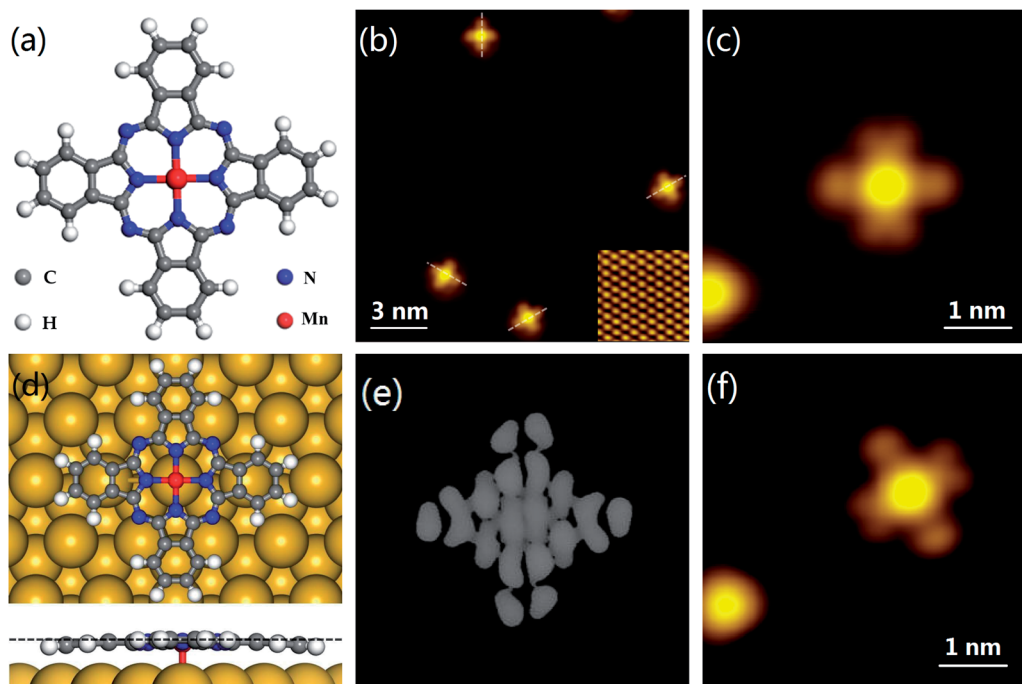


**Fig. 1** Individual MnPc molecules adsorbed on Bi(111) surface at LHe temperature. (a) Schematic structure model of the MnPc molecule; (b) STM image of isolated MnPc molecules on Bi(111),  $18.0 \text{ nm} \times 18.0 \text{ nm}$ ,  $U = 0.2 \text{ V}$ ,  $I = 60 \text{ pA}$ . The insert shows the atomic-resolution image of Bi(111) surface, where the dashed lines represent the directions of surface base vectors; (c) close-up view of a single MnPc on Bi(111),  $5.0 \text{ nm} \times 5.0 \text{ nm}$ ,  $U = 0.3 \text{ V}$ ,  $I = 50 \text{ pA}$ . (d) Top view (upper) and side view (lower) of the optimized adsorption configuration of a MnPc on Bi(111). (e) Simulated STM image of a single MnPc on Bi(111) at  $0.3 \text{ V}$ . (f) Rotation of the MnPc molecule in (c) by  $60^\circ$  driven by low-bias scanning,  $5.0 \text{ nm} \times 5.0 \text{ nm}$ ,  $U = 0.88 \text{ V}$ ,  $I = 50 \text{ pA}$ .



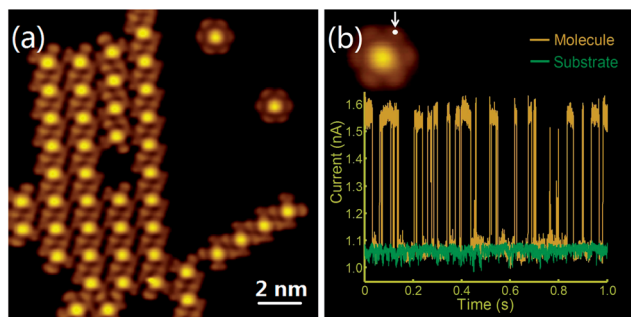


Fig. 2 (a) Coexistence of single molecular rotors and a self-assembled domain of MnPc molecules at 78 K,  $15.0 \text{ nm} \times 15.0 \text{ nm}$ ,  $U = 1.0 \text{ V}$ ,  $I = 30 \text{ pA}$ ; (b)  $I-t$  spectra acquired at bias of  $0.5 \text{ V}$  with the STM tip positioned at the white spot and over the bare Bi(111).

MnPc chains and two isolated molecules at 78 K. The MnPc molecules in the chains have a similar appearance to the molecule in Fig. 1(c). In contrast, the upper two molecules show a flower-like feature with one central protruding ball and six surrounding lobes. Such flower-like molecules are absent at LHe temperature. We propose that the flower-like feature is because of rapid rotation of the MnPc molecule.

To verify the rotation of the molecule on Bi(111), we measured  $I-t$  spectra by positioning the STM tip above the MnPc molecule with the feedback loop turned off. Fig. 2(b) shows a typical  $I-t$  spectrum of the flower-like molecule with a time interval of 5 s. The frequent changes in the tunneling current are associated with the rotation rate.<sup>18,26</sup> The  $I-t$  spectrum recorded over the bare Bi(111) surface does not show any distinct changes in the current, which excludes the possibility of impurities. Thus, the flower-like feature is caused by molecular rotation.

Similar to the case of BuSMe molecules on Cu(111),<sup>5</sup> the six lobes suggest there are energetically favorable positions for the

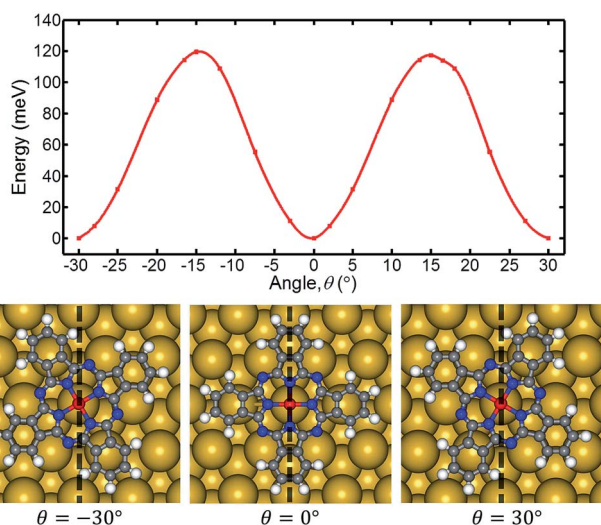


Fig. 3 Adiabatic PES plotted with spline interpolation. The points correspond to the result of DFT calculations. Geometries at azimuthal angles of  $0^\circ$ ,  $-30^\circ$ ,  $30^\circ$  are shown at the bottom.

molecule on the Bi(111) surface. Accordingly, we calculated the adiabatic potential-energy surface (PES) of the MnPc molecule as a function of the azimuthal rotation angle ( $\theta$ ).<sup>24</sup> Fig. 3 shows the PES plotted with spline interpolation. The three most stable orientations are  $\theta = 0^\circ$ ,  $-30^\circ$ , and  $30^\circ$ . The position at  $0^\circ$  corresponds to the minimum energy configuration in Fig. 1(d). After rotation of  $\pm 14.5^\circ$ , two maxima occur in the PES. From the three discrete configurations shown at the bottom of Fig. 3, it is clear that there are three equivalent adsorption orientations for MnPc on the Bi(111) surface. Thus, the flower-like feature is related to the symmetry of the MnPc molecule and hexagonal Bi(111) surface.

A potential barrier about 120 meV needs to be overcome to rotate the MnPc molecule. Because the flower-like feature does not appear at 4.6 K, it is clear that thermal energy plays a crucial role in rotating the MnPc molecule. Additionally, tunneling electrons also have the ability to drive or control molecular motions.<sup>7,17</sup> We believe that the energy from tunneling electrons is considerable in this case. The experimental and theoretical results suggest that the flower-like feature is a low-frequency image of high-frequency molecular rotation, a MnPc molecule rotates with respect to Bi(111) surface.

We also achieved the starting and stopping of MnPc rotors. As shown in Fig. 4(a), the MnPc molecule is stationary when attaching to a tetramer chain. We used the STM tip to isolate the MnPc molecule from the tetramer. As soon as it detached, the single MnPc molecule started to freely rotate on the substrate [Fig. 4(b)]. This manipulation confirms that the flower-like feature is because of rotation of the MnPc molecule on the Bi(111) surface.

Another interesting manipulation is stopping the MnPc rotors. As shown in the upper left of Fig. 5(a), two MnPc molecules initially rotated at close range. After a lateral shift, which caused by the manipulation of STM tip, the lower MnPc attached to the upper one. As soon as they were in contact, two MnPc molecules stopped to remain stationary [Fig. 5(b)]. In particular, three MnPc molecules (indicated by arrows) initially rotated on the Bi(111) surface in Fig. 5(c). A MnPc molecule with a suppressed center (marked by a circle) attached to the molecular chains. The suppression may be caused by modification of the

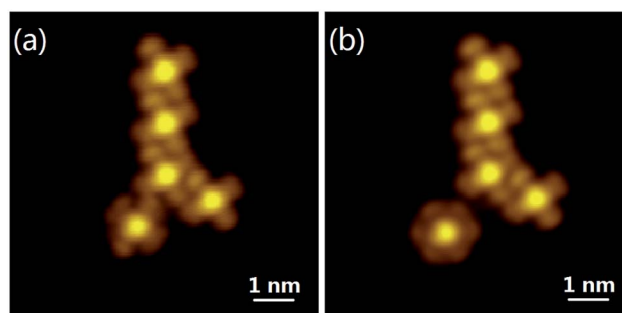
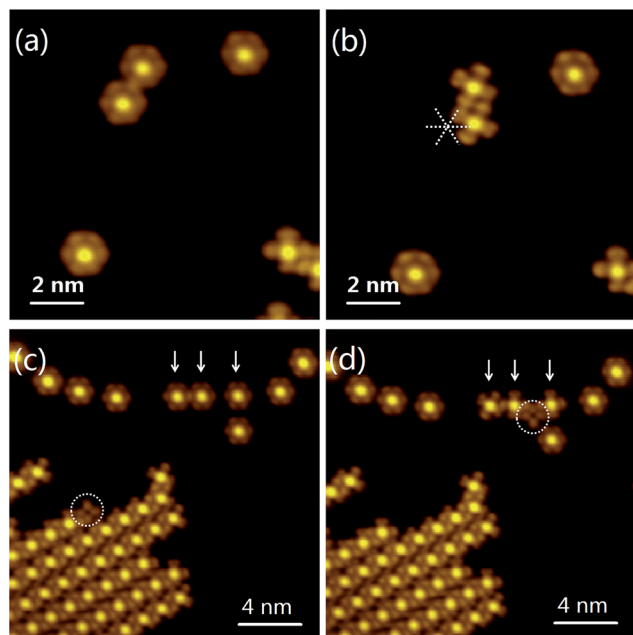


Fig. 4 A MnPc molecule rotating on the Bi(111) surface after detaching from a tetramer chain. (a) The MnPc molecule attached to a tetramer chain.  $8.0 \text{ nm} \times 8.0 \text{ nm}$ ,  $U = 0.6 \text{ V}$ ,  $I = 28 \text{ pA}$ ; (b) the MnPc molecule rotating on the substrate after detaching from the tetramer chain.  $8.0 \text{ nm} \times 8.0 \text{ nm}$ ,  $U = 0.5 \text{ V}$ ,  $I = 28 \text{ pA}$ .





**Fig. 5** Simultaneous stopping three MnPc rotors by inserting another molecule. (a) Two MnPc molecules rotating at close range.  $12.0\text{ nm} \times 12.0\text{ nm}$ ,  $U = 0.5\text{ V}$ ,  $I = 30\text{ pA}$ ; (b) stopping rotation of the two molecules by manipulating with STM tip.  $12.0\text{ nm} \times 12.0\text{ nm}$ ,  $U = 0.5\text{ V}$ ,  $I = 30\text{ pA}$ . (c) Three MnPc molecules rotating when not in contact.  $20.0\text{ nm} \times 20.0\text{ nm}$ ,  $U = 1.0\text{ V}$ ,  $I = 31\text{ pA}$ ; (d) stopping rotation of the three molecules by inserting a modified MnPc molecule.  $20.0\text{ nm} \times 20.0\text{ nm}$ ,  $U = 1.0\text{ V}$ ,  $I = 30\text{ pA}$ .

central Mn ion.<sup>32,43</sup> By manipulating the modified molecule with the STM tip, we shifted the molecule and inserted it into the interspace between two MnPc rotors. The three MnPc rotors simultaneously stopped when they formed a tetramer chain with the modified molecule [Fig. 5(d)]. These manipulations were performed by controlling the intermolecular spacing.

## 4 Conclusions

We have investigated single molecule rotors of MnPc on the Bi(111) surface by STM and first-principle calculations. The STM images show that individual MnPc molecules adsorb flat on the surface at 4.6 K. Geometry optimization reveals that two benzene rings bend, reducing the symmetry. Furthermore, a flower-like molecule is observed at 78 K. Experimental  $I-t$  spectra and theoretical adiabatic PES were determined. The combined study reveals that the flower-like feature is caused by rapid rotation of the MnPc molecule. By controlling the intermolecular spacing with a STM tip, rotation of the single molecule rotors can be started and stopped.

## Acknowledgements

This work was supported by the National Natural Science Foundation of China (Grant Nos. 11574253, 10974156, 21173170, 91121013, 11604269) and the Fundamental Research Funds for the Central Universities (XDJK2016C065, XDJK2017C064).

## References

- H. Park, J. Park, A. K. L. Lim, E. H. Anderson, A. P. Alivisatos and P. L. McEuen, *Nature*, 2000, **407**, 57–60.
- G. S. Kottas, L. I. Clarke, D. Horinek and J. Michl, *Chem. Rev.*, 2005, **105**, 1281–1376.
- T. R. Kelly, R. A. Silva, H. D. Silva, S. Jasmin and Y. J. Zhao, *J. Am. Chem. Soc.*, 2000, **122**, 6935–6949.
- M. Schliwa and G. Woehlke, *Nature.*, 2003, **422**, 759–765.
- H. L. Tierney, C. J. Murphy, A. D. Jewell, A. E. Baber, E. V. Iski, H. Y. Khodaverdian, A. F. McGuire, N. Klebanov and E. C. H. Sykes, *Nat. Nanotechnol.*, 2011, **6**, 625–629.
- N. P. M. Huck, W. F. Jager, B. de Lange and B. L. Feringa, *Science*, 1996, **273**(5282), 1686–1688.
- S. C. Yan, Z. J. Ding, N. Xie, H. Q. Gong, Q. Sun, Y. Guo, X. Y. Shan, S. Meng and X. H. Lu, *ACS Nano*, 2012, **6**, 4132–4136.
- J. Clayden and J. H. Pink, *Angew. Chem., Int. Ed.*, 1998, **37**, 1937–1939.
- P. R. Ashton, R. Ballardini, V. Balzani, I. Baxter, A. Credi, M. C. T. Fyfe, M. T. Gandolfi, M. Gómez-López, M.-V. Martínez-Díaz, A. Piersanti, N. Spencer, J. F. Stoddart, M. Venturi, A. J. P. White and D. J. Williams, *J. Am. Chem. Soc.*, 1998, **120**, 11932–11942.
- C. Joachim, H. Tang, F. Moresco, G. Rapenne and G. Meyer, *Nanotechnology*, 2002, **13**, 330–335.
- G. Jimenez-Bueno and G. Rapenne, *Tetrahedron Lett.*, 2003, **44**, 6261–6263.
- J. K. Gimzewski, C. Joachim, R. R. Schlittler, V. Langlais, H. Tang and I. Johanssen, *Science*, 1998, **281**, 531–533.
- M. Stöhr, T. Wagner, M. Gabriel, B. Weyers and R. Möller, *Phys. Rev. B: Condens. Matter Mater. Phys.*, 2001, **65**, 033404.
- D. Y. Zhong, T. Blömker, K. Wedeking, L. F. Chi, G. Erker and H. Fuchs, *Nano Lett.*, 2009, **9**, 4387–4391.
- D. Kühne, F. Klappenberger, W. Krenner, S. Klyatskaya, M. Ruben and J. V. Barth, *Proc. Natl. Acad. Sci. U. S. A.*, 2010, **107**, 21332–21336.
- L. Bartels, F. Wang, D. Möller, E. Knoesel and T. F. Heinz, *Science*, 2004, **305**, 648–651.
- N. Henningsen, K. J. Franke, I. F. Torrente, G. Schulze, B. Priewisch, K. Rück-Braun, J. Dokić, T. Klamroth, P. Saalfrank and J. I. Pascual, *J. Phys. Chem. C*, 2007, **111**, 14843–14848.
- L. Gao, Q. Liu, Y. Y. Zhang, N. Jiang, H. G. Zhang, Z. H. Cheng, W. F. Qiu, S. X. Du, Y. Q. Liu, W. A. Hofer and H. J. Gao, *Phys. Rev. Lett.*, 2008, **101**, 197209.
- N. Wintjes, D. Bonifazi, F. Y. Cheng, A. Kiebele, M. Stöhr, T. Jung, H. Spillmann and F. Diederich, *Angew. Chem.*, 2007, **46**, 4089–4092.
- K. P. Ghiggino, J. A. Hutchison, S. J. Langford, M. J. Latter, M. A. P. Lee, P. R. Lowenstern, C. Scholes, M. Takezaki and B. E. Wilman, *Adv. Funct. Mater.*, 2007, **17**, 805–813.
- A. E. Baber, H. L. Tierney and E. C. H. Sykes, *ACS Nano*, 2008, **2**, 2385–2391.
- B. V. Rao, K. Y. Kwon, A. W. Liu and L. Bartels, *J. Chem. Phys.*, 2003, **119**, 10879–10884.



- 23 D. Lensen and J. A. A. W. Elemans, *Soft Matter*, 2012, **8**, 9053–9063.
- 24 J. Schaffert, M. C. Cottin, A. Sonntag, H. Karacuban, C. A. Bobisch, N. Lorente, J. P. Gauyacq and R. Möler, *Nat. Mater.*, 2013, **12**, 223–227.
- 25 A. M. Moore, B. A. Mantooth, Z. J. Donhauser, Y. X. Yao, J. M. Tour and P. S. Weiss, *J. Am. Chem. Soc.*, 2007, **129**, 10352–10353.
- 26 A. D. Jewell, H. L. Tierney, A. E. Baber, E. V. Iski, M. Laha and E. C. H. Sykes, *J. Phys.: Condens. Matter*, 2010, **22**, 264006.
- 27 B. C. Stipe, M. A. Rezaei and W. Ho, *Science*, 1998, **279**, 1907–1909.
- 28 C. J. Murphy, Z. C. Smith, A. Pronschinski, E. A. Lewis, M. L. Liriano, C. Wong, C. J. Ivimey, M. Duffy, W. Musial, A. J. Therrien, S. W. Thomas and E. C. H. Sykes, *Phys. Chem. Chem. Phys.*, 2015, **17**, 31931–31937.
- 29 F. Chiaravalloti, L. Gross, K. H. Rieder, S. M. Stojkovic, A. Gourdon, C. Joachim and F. Moresco, *Nat. Mater.*, 2007, **6**, 30–33.
- 30 A. D. Zhao, Q. X. Li, L. Chen, H. J. Xiang, W. H. Wang, S. Pan, B. Wang, X. D. Xiao, J. L. Yang, J. G. Hou and Q. S. Zhu, *Science*, 2005, **309**, 1542–1544.
- 31 Y. S. Fu, T. Zhang, S. H. Ji, X. Chen, X. C. Ma, J. F. Jia and Q. K. Xue, *Phys. Rev. Lett.*, 2009, **103**, 257202.
- 32 L. W. Liu, K. Yang, Y. H. Jiang, B. Q. Song, W. D. Xiao, L. F. Li, H. T. Zhou, Y. L. Wang, S. X. Du, M. Ouyang, W. A. Hofer, A. H. C. Neto and H. J. Gao, *Sci. Rep.*, 2013, **3**, 1210.
- 33 P. Jiang, X. C. Ma, Y. X. Ning, C. L. Song, X. Chen, J. F. Jia and Q. Xue, *J. Am. Chem. Soc.*, 2008, **130**, 7790–7791.
- 34 Q. M. Guo, Z. H. Qin, K. Zang, C. D. Liu, Y. H. Yu and G. Y. Cao, *Langmuir*, 2010, **26**, 11804–11808.
- 35 R. A. Rehman, W. D. Dou, H. Q. Qian, H. Y. Mao, F. Floether, H. J. Zhang, H. Y. Li, P. He and S. N. Bao, *Surf. Sci.*, 2012, **606**, 1749–1754.
- 36 G. Kresse and J. Hafner, *Phys. Rev. B: Condens. Matter Mater. Phys.*, 1994, **49**, 14251.
- 37 G. Kresse and J. Furthmüller, *Phys. Rev. B: Condens. Matter Mater. Phys.*, 1996, **54**, 11169.
- 38 J. P. Perdew, J. A. Chevary, S. H. Vosko, K. A. Jackson, M. R. Pederson, D. J. Singh and C. Fiolhais, *Phys. Rev. B: Condens. Matter Mater. Phys.*, 1992, **46**, 6671–6687.
- 39 P. E. Blöchl, *Phys. Rev. B: Condens. Matter Mater. Phys.*, 1994, **50**, 17953.
- 40 G. Kresse and D. Joubert, *Phys. Rev. B: Condens. Matter Mater. Phys.*, 1999, **59**, 1758.
- 41 S. Grimme, *J. Comput. Chem.*, 2006, **27**, 1787–1799.
- 42 J. Tersoff and D. R. Hamann, *Phys. Rev. Lett.*, 1983, **50**, 1998–2001.
- 43 Y. F. Wang, J. Kröger, R. Berndt and W. A. Hofer, *J. Am. Chem. Soc.*, 2009, **131**, 3639–3643.
- 44 S. Javaid, S. Lebègue, B. Detlefs, F. Ibrahim, F. Djeghloul, M. Bowen, S. Boukari, T. Miyamachi, J. Arabski, D. Spor, J. Zegenhagen, W. Wulfhekel, W. Weber, E. Beaurepaire and M. Alouani, *Phys. Rev. B: Condens. Matter Mater. Phys.*, 2013, **87**, 155418.

